

Rhodobacter sphaeroides Phosphoribulokinase: Identification of Lysine-165 as a Catalytic Residue and Evaluation of the Contributions of Invariant Basic Amino Acids to Ribulose 5-Phosphate Binding[†]

Jennifer A. Runquist, David H. T. Harrison, and Henry M. Miziorko*

Department of Biochemistry Medical College of Wisconsin, Milwaukee, Wisconsin 53226

Received May 5, 1999; Revised Manuscript Received July 9, 1999

ABSTRACT: *Rhodobacter sphaeroides* phosphoribulokinase (PRK) is inactivated upon exposure to pyridoxal phosphate/sodium borohydride, suggesting a reactive lysine residue. Protection is afforded by a combination of the substrate ATP and the allosteric activator NADH, suggesting that the targeted lysine maps within the active site. PRK contains two invariant lysines, K53 and K165. PRK–K53M retains sensitivity to pyridoxal phosphate, implicating K165 as the target of this reagent. PRK–K165M retains wild-type structure, as judged by titration with effector NADH and the tight-binding alternative substrate trinitrophenyl–ATP. The catalytic activity of K165M and K165C mutants is depressed by $>10^3$ -fold. Residual activity of K165M is insensitive to pyridoxal phosphate, confirming K165 as the target of this reagent. The decreased catalytic efficiency of K165 mutants approaches the effect measured for a mutant of D169, which forms a salt-bridge to K165. K165M exhibits a 10-fold increase in $S_{1/2}^{ATP}$ and a 10^2 -fold increase in K_m^{Ru5P} . To evaluate the contribution to Ru5P binding of K165 in comparison with this substrate's interaction with invariant H45, R49, R168, and R173, PRKs mutated at these positions have been used to determine relative K_i values for 6-phosphogluconate, a competitive inhibitor with respect to Ru5P. Elimination of the basic side chain of K165, R49, and H45 results in increases in K_m^{Ru5P} which correlate well with the magnitude of increases in $K_i^{6-phosphogluconate}$. In contrast, while mutations eliminating charge from R168 and R173 result in enzymes with substantial increases in K_m^{Ru5P} , such mutant enzymes exhibit only small increases in $K_i^{6-phosphogluconate}$. These observations suggest that K165, R49, and H45 are major contributors to Ru5P binding.

Phosphoribulokinase (PRK¹; EC 2.7.1.19) catalyzes the in-line transfer (1) of the γ -phosphoryl group of ATP to the C1-hydroxyl of ribulose 5-phosphate (Ru5P) to form ribulose 1,5-bisphosphate (2), the CO₂ acceptor of the reductive pentose phosphate pathway. A variety of solution state approaches, including protein modification and site-directed mutagenesis, have been employed to identify amino acids involved in regulation (3–5), substrate binding (6, 7), or catalysis (8, 9). A high-resolution structure of the *Rhodobacter sphaeroides* protein has recently become available (10). The enzyme folds similarly to the nucleotide monophosphate kinase family of proteins (11, 12). Catalysis of phosphoryl transfer by enzymes that exhibit the nucleotide monophosphate kinase fold is usually supported by multiple positively charged amino acids. This observation seems to be valid regardless of whether these enzymes catalyze

phosphoryl transfer between two nucleotides (13) or between a nucleotide donor and a nonnucleotide acceptor metabolite (14).

The structure available for PRK represents an “open” form of the enzyme, with no ligands bound at catalytic or effector sites. Thus, it provides only limited insight into the substrate–protein interactions that account for catalysis. To progress toward a more complete identification of active site amino acids that support catalysis, we have diagnosed and eliminated a barrier that previously impeded productive affinity labeling of the active site of *R. sphaeroides* PRK, implicated a reactive lysine as being situated within the active site and tested the functional consequences of the elimination of this residue's positive charge. The results of these studies are presented in this report and interpreted within the context of the consensus that emerges for the nucleotide monophosphate kinase fold proteins. A preliminary account of this study has appeared (15).

MATERIALS AND METHODS

Materials. Deoxyoligonucleotides and fluorescein-labeled sequencing primers were purchased from Operon Technologies, Inc. T4 DNA ligase was purchased from New England Biolabs. Restriction enzymes were obtained from both New England Biolabs and Pharmacia Biotech. Isolation of plasmid DNA grown in *Escherichia coli* JM105 was accomplished

[†] This work was supported, in part, by a Herman–Frasch Foundation award to D. H. T. H. and by a grant from USDA (NRI–CRG/Photosynthesis) to H. M. M.

* Address correspondence to: Henry M. Miziorko, Department of Biochemistry, Medical College of Wisconsin, 8701 Watertown Plank Rd., Milwaukee, WI 53226. Telephone: 414-456-8437. Fax: 414-456-6570. E-mail: miziorko@mcw.edu.

¹ Abbreviations used are: PRK, phosphoribulokinase; Ru5P, ribulose 5-phosphate; RuBP, ribulose 1,5-bisphosphate; TNP-ATP, 2'(3')-O-(2, 4, 6-trinitrophenyl) adenosine 5'-triphosphate; IPTG, isopropyl thiogalactoside; PLP, pyridoxal phosphate.

using Sigma's Plasmid Pure(TM) miniprep Kit, and Qiagen's Plasmid Mini and Midi Kits. Isolation of DNA fragments was accomplished using a QIAEX II Gel Extraction Kit. DNA sequence analysis was performed using a Thermo Sequenase Core Sequencing Kit from Amersham Life Sciences and a Pharmacia/LKB A. L. F. DNA sequencer.

For recombinant protein expression, ampicillin was purchased from Fisher Scientific and isopropyl β -D-thiogalactoside (IPTG) from Research Products International. Adenosine 5'-triphosphate, cystamine diHCl, 2-mercaptoethanol, β -NADH, 6-phosphogluconate, pyridoxal phosphate, D-ribulose 5-phosphate, DTT, reactive green-19 agarose, and Tris buffer were obtained from Sigma Chemical Co. Hepes buffer was obtained from Research Organics, 2-bromoethylamine HBr from Aldrich Chemical, sodium ^{14}C bicarbonate, 56 mCi/mM, from American Radiolabeled Chemicals, and Q Sepharose Fast Flow from Pharmacia Biotech. For fluorescence experiments, TNP-ATP [2'(3')-O-(2,4,6-trinitrophenyl)adenosine 5'-triphosphate] was supplied by Molecular Probes. The *Rhodospirillum rubrum* RuBP carboxylase required for the ^{14}C CO₂ fixation assay of PRK activity was isolated after expression in *E. coli* JM103 using a plasmid generously provided by C. R. Somerville (35).

Construction of prkA Mutant Alleles. The mutant alleles of prkA encoding the single amino acid substitutions K165M and K165C were constructed in pETbprkwt and pETbprkwtC194A (which encodes an active, cysteine-free PRK), respectively, using cassette mutagenesis and a three-way ligation strategy previously described (8). For K165M, AAG was changed to ATG using the mutagenic oligonucleotide: 5'-GATCCAGATGATCCACCGCGACCG-3'. For the K165C mutation, AAG was changed to TGC using the mutagenic oligonucleotide: 5'-GATCCAGTGCATCCACCGCGACCG-3'. Potentially mutagenic plasmids were screened to verify that the appropriate restriction enzyme sites were still intact. DNA sequencing, in both directions, confirmed that the expression plasmids encoded the anticipated methionine or cysteine mutations and verified that no additional mutations had been introduced.

Expression and Purification of PRK. *E. coli* BL21(DE3) cultures containing plasmids pETbprkK165M and pETbprkC194A/K165C were grown at 25 °C in 2 L of ampicillin-containing LB media to an OD₆₀₀ ~0.7. Expression of PRK was induced by addition of IPTG to a final concentration of 1 mM followed by 3–4 h of additional growth. The cells were collected by low-speed centrifugation; cell pellets were suspended and disrupted using a French pressure cell. For isolation of PRK (8, 25), a 100 000 g supernatant was prepared and subjected to Q-Sepharose anion exchange chromatography followed by affinity chromatography on reactive green-19 agarose. PRK was eluted from reactive green-19 agarose affinity resin with a buffer containing 25 mM Tris-HCl (pH 8.2), 10 mM 2-mercaptoethanol, 1 mM EDTA, and 10 mM ATP. Alternatively, elution was performed with 10 mM 2-mercaptoethanol, 1 mM EDTA, and 1 M KCl to ensure that no ATP would remain bound to isolated enzyme. For quantitative protein concentration estimates, an extinction coefficient of 50 303 M⁻¹ cm⁻¹ at 280 nm was used (16). Protein concentration was also determined by the method of Bradford (17) using bovine serum albumin as a standard with an appropriate correction

in conversion to the spectrophotometrically determined estimate.

TNP-ATP and NADH Binding Stoichiometry Measurements. TNP-ATP binding to PRK was followed by measurements of fluorescence enhancement (at 545 nm), utilizing a SLM 4800C spectrofluorometer as described previously (16). NADH binding to PRK was also measured using fluorescence enhancement at 440 nm. The binding stoichiometry of mono- and dinucleotides to PRK was determined from the intersection point of lines fit to the low-occupancy and plateau regions of the titration curves by linear regression. Calculated stoichiometries reflect binding sites per 32 kDa PRK subunit.

Kinetic Characterization of PRK. A radioisotopic assay that involves trapping the PRK reaction product RuBP via the RuBP carboxylase-dependent incorporation of ^{14}C CO₂ to form acid-stable [^{14}C]-3-phosphoglycerate (18) was utilized. In standard assays, the final concentrations of reaction mixture components were 100 mM Hepes (pH 8.0), 1 mM DTT, 20 mM MgCl₂, 20 mM KH¹⁴CO₃ (~1000 dpm/nmol), 5 mM ATP, 1 mM Ru5P, 1 mM NADH, and 100 milliunits of recombinant RuBP carboxylase. Enzyme assays were conducted at 30 °C. For kinetic characterization of the mutant proteins, ATP concentration ranges varied from 0.05 to 15 mM; Ru5P concentration ranges varied from 0.05 to 8 mM. Kinetic data were fit by a nonlinear regression analysis algorithm (19).

Inactivation of PRK with Pyridoxal Phosphate. For wild-type PRK or K53M, the PLP inactivation reaction was carried out at 25 °C by incubation of enzyme (0.5 nmol) in 50 μL of 50 mM Hepes buffer (pH 7.9) and 10 mM MgCl₂. PLP (50–400 μM , as indicated in Table 1) was added to the enzyme solution at zero time. Aliquots were removed from the inactivation mixture after twenty-five minutes and reduced with ice-cold NaBH₄ (final concentration 5 mM in 10 mM Na₂CO₃). After 5 min of reduction, the enzyme was diluted 300-fold into the assay mixture and activity was spectrophotometrically determined. As a control, a sample of PRK was incubated with borohydride only; control activity was equivalent to untreated enzyme. Because of the low activity of the K165M mutant, PLP inactivation was monitored using the radioactive assay. Mutant enzyme (0.85 nmol; 17 μM) was added to the inactivation mixtures, which included concentrations of PLP from 50 μM to 1 mM. After 25 min, the reaction was terminated by borohydride reduction and activity was measured by 10-fold dilution of appropriate aliquots into the radioactive assay solution. Borohydride controls showed that the concentrations of the reductant used did not significantly affect the radioactive assay.

Inhibition of PRK with 6-Phosphogluconate. Inhibition studies were accomplished using the radioactive assay. Samples contained concentrations of phosphogluconate ranging from 0.1 to 25 mM, as appropriate for wt PRK and each of the 5 mutants that exhibit an inflated $K_{\text{m Ru5P}}$ (K165M, R49Q, H45N, R168Q, and R173Q). For K_i determinations, kinetic data were analyzed by nonlinear regression analysis, using the EZ-FIT program (20).

RESULTS

Development of a system for overexpression of *R. sphaeroides* PRK (8) together with the productive application

Table 1: Pyridoxal Phosphate Inhibition of PRK and Protection in Binary and Ternary Complexes^a

enzyme sample	incubation mix components	% activity remaining
wild-type PRK	minus PLP	100
	PLP (50 μ M)	10
	PLP + NADH (1.0 mM)	10
	PLP + Ru5P (1.0 mM)	20
	PLP + ATP (2.0 mM)	23
K53M	PLP + NADH + ATP	100
	minus PLP	100
	PLP (50 μ M)	15
K165M	PLP (50 μ M) ^b	101

^a The percent activity remaining after a 25 min incubation with or without 50 μ M PLP is indicated. The PLP-containing inactivation mix was quenched with sodium borohydride. For wild-type and K53M PRKs, activity was assayed after dilution of a sample aliquot into a coupled spectrophotometric assay mixture as described in Materials and Methods. For K165M PRK, the radioactive assay was used. ^b For K165M, additional incubations at PLP concentrations of 100, 200, and 400 μ M did not reduce activity below 93%.

of affinity chromatography (21) to isolate enzyme from bacterial extracts has tremendously expedited the use of bacterial PRK as a model for investigation of enzymatic catalysis and allosteric regulation. Nonetheless, the seminal protein modification work was performed on preparations of the plant protein (3, 22, 23, 24). Several reagents that productively modify the plant enzyme are relatively inefficient for inactivation of affinity-isolated bacterial PRK. In retrospect, this may be due to the formation, during affinity isolation, of a stable PRK–ATP complex that resists modification (particularly by reactive ATP analogues). The subsequent development of a protocol for isolation of ATP-free *R. sphaeroides* PRK (25) allowed reevaluation of the utility of protein modification in identifying active site amino acids.

Pyridoxal Phosphate Inactivation of PRK. The lysine-specific reagent, pyridoxal phosphate, can selectively modify phosphoryl transfer enzymes, presumably due to the specificity of interaction afforded by its phosphoryl moiety (26). Upon incubation with a low concentration (50 μ M) of pyridoxal phosphate, *R. sphaeroides* PRK loses activity in a time-dependent fashion; borohydride reduction is required to accomplish irreversible inactivation, presumably due to reduction of a Schiff's base adduct between reagent and a lysine residue. After a 25 min. incubation, initial PRK activity is reduced by an order of magnitude (Table 1). Protection against inactivation was not afforded at any substantial level (Table 1) by the individual addition of either the positive effector NADH (1.0 mM) or the phosphoryl donor substrate, ATP (2.0 mM). These concentrations are adequate to saturate enzyme sites based on the observed ability of each of these metabolites to form tight binary complexes with isolated PRK (16). Similarly, levels of Ru5P (1.0 mM) sufficient to saturate enzyme sites offered little protection against pyridoxal phosphate. Only upon the combined addition of NADH and ATP to the incubation mix was pyridoxal phosphate inactivation impeded; indeed, this combination affords complete protection (Table 1). Under steady-state turnover conditions, NADH markedly influences active site occupancy by the nucleotide substrate, lowering by more than an order of magnitude the concentration of ATP required to saturate PRK (16). This observation prompts interpretation of the inactivation

	165	168	173	
arabprk	KFAWK	IQRDM	AERGH	SLES
whtprk	KFAWK	IQRDM	AERGH	SLES
mescrprk	KFAWK	IQRDM	AERGH	SLES
spprk	KFAWK	IQRDM	KERGH	SLES
cprk	KFAWK	IQRDM	AERGH	SLES
sycprk	KINWK	IQRDM	AERGH	TYED
rsprk1	EWIQK	IHRDR	ATRGY	TTEA
rsprk2	EWIQK	IHRDR	AQRGY	TTEA
aeprk1	EWIQK	LWRDK	KQRGY	STEA
aeprk2	EWIQK	LWRDK	KQRGY	STEA
nitroprk	EWIQK	LHRDR	NARGY	STEA
xflavusprk	EWIQK	IHRDK	ATRGY	TTED

FIGURE 1: Alignment of residues 161–179 from deduced PRK sequences. Invariant basic amino acids (K165, R168, and R173) are indicated in boldface. The alignment of these residues is extracted from sequences documented in a previous report (8). Abbreviations used are: arab, *Arabidopsis*; wht, *Triticum aestivum*; mescr, *Mesembryanthemum crystallinum*; sp, *Spinacea oleracea*; c, *Chlamydomonas reinhardtii*; syc, *Synechocystis*; rs, *Rhodobacter sphaeroides*; ae, *Alcaligenes eutrophus*; nitro, *Nitrobacter vulgaris*; xflavus, *Xanthobacter flavus*.

tion data summarized in Table 1 to support the hypothesis that pyridoxal phosphate's target is situated within the active site of PRK.

Strategy for Identification of an Active Site Lysine in PRK. PRK exists within a wide collection of prokaryotes and eukaryotes; alignment of the various deduced PRK sequences suggests that there are only two lysines (K53, K165) that qualify as highly conserved, an attribute expected of an active site amino acid. While K165 is invariant (Figure 1) in the PRK sequences currently available, K53 is replaced by arginine in PRKs from *Nitrobacter* and *Xanthobacter flavus*; this conservative substitution by another basic residue does not necessarily preclude analogous function by the side chain of residue 53 in these two PRKs. Previously, we employed site-directed mutagenesis to evaluate the function of K53, since the corresponding residue (K68 of spinach PRK) is modified by the affinity label adenosine triphosphopyridoxal (24). Thus, purified K53M PRK, which has been kinetically characterized as substantially retaining wild-type PRK traits, was available for a test of sensitivity to pyridoxal phosphate modification. This mutant enzyme, which lacks a modification target at residue 53 but retains lysine at residue 165, is inactivated comparably to wild-type PRK (Table 1). The

Table 2: Substrate and Effector Binding by PRK Mutants

enzyme	$n_{\text{TNP-ATP}}^a$	n_{NADH}
wild-type	1.0 ± 0.03	0.97 ± 0.03
K165M	0.85 ± 0.09	0.76 ± 0.06
K165C	0.87 ± 0.08	0.83 ± 0.03

^a n denotes the calculated number of binding sites per enzyme subunit. Stoichiometries for TNP-ATP and NADH binding were determined from fluorescence titrations as described in Methods.

collected data imply that K165 is likely to be the active site PRK residue, which is sensitive to modification. On this basis, a more detailed investigation of a PRK variant lacking K165 seemed to be well-justified.

Properties of PRK K165 Mutants. Plasmids encoding K165M and K165C substitutions were used to transform *E. coli* BL21; IPTG induced mutant PRK protein expression, which occurred at rates and levels comparable to those observed with wild-type enzyme. Using methodology previously documented for preparing wild-type and other mutant PRKs that either lack or contain tightly bound ATP (8, 25), K165M and K165C mutant proteins were purified from bacterial extracts to a high degree of homogeneity and with yields comparable to the recovery reported for wild-type PRK. To ensure that the mutant PRKs retain substantial structural integrity (and are, therefore, useful for detailed characterization), the binding of the fluorescent alternative substrate TNP-ATP was evaluated. As documented in Table 2, titrations of K165M and K165C proteins indicate binding stoichiometries that approximate the value measured for wild-type PRK. Likewise, fluorescence titrations of these mutant proteins with the positive allosteric effector, NADH, indicate that they substantially retain the binding characteristics that wild-type enzyme exhibits for this activator (Table 2). The K165M and K165C mutants form stoichiometric levels of tight binary complexes not only with the nucleotide substrate but also with the allosteric effector. This argues that despite their diminished activity (Table 3), the catalytic and regulatory sites of these mutants are not substantially different from wild-type PRK. It follows that overall tertiary structure of the mutant PRKs is also unperturbed. In this context, it is significant that when ATP-free K165M (prepared by salt elution of reactive green-19 agarose affinity resin) is incubated with pyridoxal phosphate under conditions that result in substantial inactivation of wild-type enzyme and the PRK mutant K53M, there is no substantial effect on the residual K165M activity (Table 1). This observation validates the hypothesis that K165 is situated within the active site of PRK and accounts for the sensitivity of wild-type enzyme to pyridoxal phosphate.

Despite the fact that K165 is the likely target of pyridoxal phosphate modification, it should not be presumed that the side chain of a residue situated at this location will invariably be reactive. In attempts to partially restore catalytic activity, K165C was incubated with either 100 mM 2-bromoethylamine (50 mM Tris-Cl, pH 8.2; 8 h) or 125 mM cystamine (in 50 mM Tris-Cl, pH 8.0; 8 h or 24 h). Alkylation by the former reagent or disulfide exchange by the latter reagent would modify C165 to restore a positive charge at this position in the mutant protein. Neither of these incubations restored activity to K165C.

Kinetic Characterization of PRK K165 Mutants. The hypothesis that K165 is an active site residue is supported

by the results of the kinetic characterization of K165M and K165C. While significant differences between wild-type and K165 mutants are observed not only for V_{max} but also for each of the K_{m} parameters (Table 3), the 3 orders of magnitude diminution in V_{max} dominates any comparison and argues that K165 strongly influences catalysis. In the context of ATP saturation, which exhibits a sigmoidal dependence, the mutants exhibit an order of magnitude increase in $S_{1/2}$ but not a significant change in the Hill coefficient. This perturbation is modest in comparison with the effect on $K_{\text{m Ru5P}}$, which increases by 2 orders of magnitude in comparison with the value for wild-type enzyme (Table 3). The $K_{\text{m Ru5P}}$ data for K165M, like those for wild-type PRK, are best fit to a hyperbolic curve. In the case of K165C, the best fit for the Ru5P saturation data is obtained using a curve with a slightly sigmoid trait (Hill coefficient, $n_{\text{H}} = 1.28$) but the $S_{1/2}$ value (11.0 mM) is not appreciably different from the $K_{\text{m Ru5P}}$ (10.3 mM) measured for the K165M data.

Inhibition of Wild-type and Mutant PRKs by 6-Phosphogluconate. In earlier studies, $K_{\text{m Ru5P}}$ perturbations have been observed as dominant effects of mutations and have been assumed to reflect changes in binding affinity for Ru5P (6, 7). In the case of the K165 mutations, the kinetic data reflect both a large perturbation in V_{max} and a smaller but substantial increase in $K_{\text{m Ru5P}}$, complicating any interpretation and suggesting that it would be useful to determine the relative contributions of catalytic and binding parameters to the measured $K_{\text{m Ru5P}}$. Unlike K_{m} comparisons of wild-type and mutant enzymes, which may be complicated by changes in both catalytic and binding terms, K_{i} comparisons should reflect only differences in binding affinity. For this reason, inhibition of PRK by 6-phosphogluconate, reported to be competitive with respect to Ru5P on the basis of studies using spinach chloroplast preparations (27), has been measured for isolated wild-type *R. sphaeroides* PRK (Figure 2). The results demonstrate that, for bacterial PRK, phosphogluconate is a competitive inhibitor with respect to Ru5P ($K_{\text{i}} = 222 \mu\text{M}$). Extension of these inhibition studies to the K165 mutants, as well as other PRK mutants that exhibit inflated $K_{\text{m Ru5P}}$ values (6, 9) has been performed in order to determine if they exhibit increases in K_{i} for phosphogluconate and how well the magnitude of such increases correlates with the inflation of $K_{\text{m Ru5P}}$ values that has been reported. Table 4 summarizes the results of these investigations, which reflect substantial increases in K_{i} values for H45N, K165M, and R49Q of magnitudes (~ 12 – 90 -fold) which approximate the magnitudes of the corresponding inflations (~ 40 – 200 -fold) in $K_{\text{m Ru5P}}$ values. These observations are most obviously explained by changes in binding properties of these mutants that are reflected in both Michaelis and inhibitor constants. In contrast, the changes in K_{i} values for R168Q and R173Q are small (2–5-fold increases) in comparison with the magnitude of increases in $K_{\text{m Ru5P}}$ that have been reported (~ 45 – 100 fold), suggesting that a combination of catalytic contributions and binding effects influence those $K_{\text{m Ru5P}}$ values. On the basis of this analysis of the correlation of mutations at various loci with changes in the affinity for the competitive inhibitor, phosphogluconate, it appears that the positively charged side chains of K165, R49, and H45 are major contributors to sugar phosphate binding at the active site of PRK.

Table 3: Steady-State Kinetic Parameters^a of Wild-Type and Mutant PRKs

enzyme	K_m Ru5P (mM)	n_H	$S_{1/2}$ ATP (mM)	n_H	V_{max} (units/mg)
wild-type	0.096 ± 0.014	(h)	0.55 ± 0.16	1.98 ± 0.15	338 ± 18
K165M	10.3 ± 1.4	(h)	4.28 ± 0.51	2.22 ± 0.55	0.118 ± 0.011
K165C	11.0 ± 2.2^b	1.28 ± 0.14	5.80 ± 0.93	1.80 ± 0.44	0.175 ± 0.07

^a The K_m Ru5P is the ribulose 5-phosphate concentration at half-maximal velocity, as calculated from a nonlinear regression fit of the Ru5P saturation data to the Michaelis–Menten equation. The $S_{1/2}$ ATP is the ATP concentration at half-maximal velocity, as calculated from a fit of the ATP saturation data to the Hill equation. n_H is the Hill constant. (h) indicates that the kinetics are hyperbolic with respect to Ru5P. The maximal velocity, given in micromoles per minute per milligram, is estimated from the Michaelis–Menten equation fit to the Ru5P saturation data. ^b This estimate represents $S_{1/2}$ Ru5P.

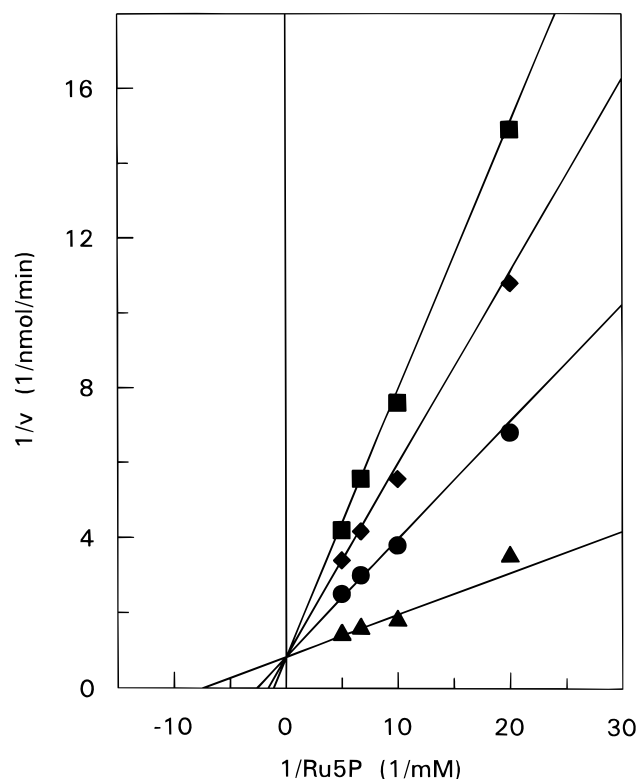


FIGURE 2: Double-reciprocal plot of the initial velocity for PRK formation of RuBP as a function of Ru5P concentration, measured at different levels of the inhibitor 6-phosphogluconate. Reaction rates were measured using the radioactive assay, as described in Methods. 6-Phosphogluconate concentrations utilized were (Δ) 0.0 mM, (\bullet) 0.4 mM, (\blacklozenge) 0.8 mM, and (\blacksquare) 1.2 mM. The data are shown fit to a competitive model using the EZFIT computer program (20) as discussed in Materials and Methods.

Table 4: 6-Phosphogluconate Inhibition of Wild-type and Mutant PRKs

enzyme	K_m Ru5P (mM)	K_i (mM) ^a
WT	0.1^b	0.222 ± 0.023
R168Q	4.6 ± 0.8^c	0.415 ± 0.032
R173Q	10.5 ± 1.5^c	1.15 ± 0.066
H45N	4.3^b	2.81 ± 0.34
R49Q	20.0^b	19.8 ± 1.93
K165M	10.3 ± 1.4	11.0 ± 1.99

^a Procedures for K_i phosphogluconate determinations are described in Methods. ^b Data taken from Sandbaken *et al.*⁶ ^c Data taken from Runquist *et al.*⁹

DISCUSSION

In the PRK structure that has recently become available, the enzyme exists in an “open” form without any bound substrates or analogues (10). The observed fold of this protein places it into the nucleotide monophosphate kinase family,

which allows a reasonable prediction of the location of the ATP binding site (11) and provides precedent (12) to suggest that the “lid” regions will contribute to the active site. The available mutagenesis evidence suggests that invariant lid residues, such as R168, D169, and R173, do indeed participate in the reaction. On the basis of the data presented above, K165 must be added to the roster of active site residues and its functional contribution evaluated. In the open form of PRK (Figure 3), a sulfate is positioned where the phosphoryl of Ru5P has been proposed to bind (10); invariant K165 as well as H69 and R186 (which are conserved only among prokaryotic PRKs) bind to sulfate. If bound sulfate indicates the sugar phosphate site, then the disruption of Ru5P binding upon elimination of the positive charge at residue 165 would not be a surprising outcome. Alternatively, the existence of a salt bridge between K165 and D169 (which has a profound influence on k_{cat} ; (8)) argues that elimination of charge at residue 165 would alter orientation of these side chains and could diminish catalytic efficiency. Since both of these contrasting functional predictions are based on an “open” structure, they had to be regarded with some caution until empirically tested. The need for such a test of function, together with the protein chemistry-based argument for the participation of a lysine in catalysis, established a strong rationale for the kinetic characterization reported here. The results allow an evaluation of the influence of K165’s positively charged side chain on steady-state turnover, during which the enzyme must assume the “closed” (i.e., substrate occupied) form.

The observation of substantial changes in multiple kinetic parameters (k_{cat} , K_m Ru5P, and K_m ATP) upon elimination of charge at position 165 complicates functional assignment. In particular, PRK’s K_m Ru5P is significantly influenced by substitutions that eliminate positive charge not only at K165 but also at each of four additional invariant residues (H45, R49, R168, R173; (6, 9)). Anchoring of phosphorylated metabolites within an active site is frequently efficiently accomplished via interaction of the phosphoryl group with *only three* positively charged side chains (28, 29). These contrasting observations underscore the potential danger inherent in the commonplace extrapolation from K_m effects to binding interactions. Thus, it seemed worthwhile to identify another approach that would afford more confidence in discriminating between these five basic residues when making functional assignments of PRK’s sugar phosphate binding residues.

The contribution of only binding terms to straightforwardly measurable inhibitor constants made attractive a survey of K_i values for these various mutant PRKs. The major limitation of this approach derives from the documentation of few metabolites with high affinity for PRK’s Ru5P site.

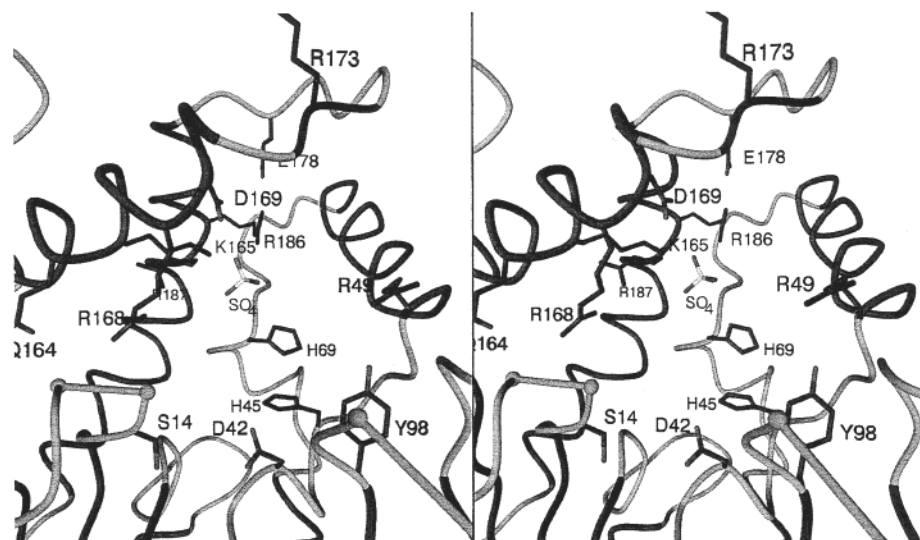


FIGURE 3: Structural representation of the *R. sphaeroides* PRK active site. Amino acids (e.g., K165, R49, and H45) that are candidates for binding Ru5P are indicated. Also shown are the putative general base catalyst (D42), sulfate ligands (H69, R186), and other active site residues implicated in previous studies (6, 8, 16).

While phosphogluconate represents the best inhibitor that has been reported, its binding to wild-type PRK is sufficiently modest that measurement of diminished affinity for mutant PRKs becomes technically difficult. The competitive inhibition approach has, nevertheless, been successfully used to underscore the importance of K165 and R49 to Ru5P binding. The importance of H45 to Ru5P binding has also been confirmed. While histidine anchors the binding of a substrate phosphoryl group to phosphofructokinase (28), there is also good precedent with phosphogluconate dehydrogenase (29) for the ability of histidine to interact with hydroxyl groups of sugar phosphates. Thus, any attempt to discriminate between whether PRK's H45 supports Ru5P binding by interaction with the phosphoryl or hydroxyl groups would be quite speculative. In contrast, given the ample precedent for arginine interactions with phosphoryl groups, functional assignment of R49, which selectively influences K_m Ru5P and K_i phosphogluconate, is most straightforwardly accomplished by proposing an interaction with Ru5P's C5 phosphoryl group. Prediction of the precise role of K165 in Ru5P binding requires a more careful analysis. The impact of K165 on Ru5P and phosphogluconate binding seems quite clear, but whether interaction involves the C1 or the phosphoryl group is less obvious. As discussed below, the influence of K165 on k_{cat} must also be accommodated in any functional assignment.

The dominant effect of eliminating K165's charged side chain is a 10^3 fold diminution in k_{cat} . This effect is more difficult to explain than K165's substrate binding function. A salt bridge exists between K165 and D169 in the open form of PRK. This observation might tempt speculation that the three to 4 orders of magnitude k_{cat} effects that are observed upon a substitution that eliminates charge from either of these side chains are attributable to the need for their precise orientation as they support transfer of ATP's γ -phosphoryl to Ru5P's C1 hydroxyl. Given the assignment of invariant D42 as the general base catalyst (8) and the more recent recognition of invariant E131 as the source of a Walker B motif carboxyl (9) that typically binds to the cation of the M^{2+} -ATP substrate, a specific role as well as the

need for precise positioning of invariant D169 becomes less clear. If the salt bridge to K165 persists when substrates bind to PRK, then perhaps the main function of D169 involves positioning of this lysine.

In the case of fructose 6-phosphate 2-kinase, the ϵ -amino group of a lysine in the lid helix region interacts with the ATP phosphoryl oxygens (14). Mutagenesis of this lysine (30) has little impact on K_m ATP; a large increase in K_m of the phosphoryl acceptor and a large diminution in k_{cat} are reported. These effects are analogous to the pattern documented here for PRK's K165. If K165 is proposed to participate in anchoring Ru5P to PRK by interacting with the C1-hydroxyl of the phosphoryl acceptor, rather than the C5 phosphoryl group, its influence on catalysis would be explained. Such an assignment would demand that under steady-state turnover conditions K165 must also be closely juxtaposed to ATP's γ -phosphoryl oxygens, a possibility well-supported by the fructose 6-phosphate 2-kinase precedent. The possibility that K165 can interact with ATP's phosphoryl oxygens is even more directly supported by mutagenesis work on spinach PRK (31) which demonstrates that W \rightarrow A substitution at the residue corresponding to prokaryotic PRK's W162 weakens ATP affinity (presumably by eliminating a stacking interaction between indole and adenine rings). If W162 is juxtaposed to ATP's purine moiety, then it is quite plausible that K165 may interact with one of its phosphoryl groups.

For adenylate kinase, where R132 maps in the lid helix, as does PRK's K165. It has been demonstrated (32) that R \rightarrow M substitution results in $>10^3$ -fold decrease in k_{cat} but little change in K_m for substrates. On this basis, R132 has been proposed to stabilize the transition state (32); a similar assignment might be considered for PRK's K165. However, any assignment based on this analogy must be viewed cautiously since phosphoryl transfer between nucleotides may proceed by an associative mechanism and require interactions between multiple basic residues and the negatively charged atoms of the nucleotide triphosphate (33). In contrast, it has been proposed that phosphoryl transfers from ATP to the hydroxyl group of other classes of metabolites involves a

dissociative transition state (34). The dissociative mechanism need not involve interactions with such an extensive array of basic amino acids.

If speculation concerning K165's interaction with Ru5P's C1 substituent and H45's interaction with the substrate's hydroxyl groups should prove to be correct, participation of other charged residues that join R49 in binding to the C5 phosphoryl group would have to be invoked. Given the modest diminution in efficacy of phosphogluconate inhibition upon replacement of R173, this residue is less obviously a candidate for such a binding assignment. Other invariant charged amino acids, while situated far from bound sulfate in the open PRK structure currently available, may need to be considered in the context of Ru5P binding. For example, R49 is not closely juxtaposed to bound sulfate or to K165 in the open PRK structure, yet both residues clearly are important to Ru5P binding and must be in close proximity during the catalytic process. The large movement in the lid regions of nucleotide monophosphate kinase fold proteins that invariably occurs upon binding of substrates (12) is expected to closely juxtapose key binding residues that may be separated by substantial distances in the open form of such proteins.

REFERENCES

- Miziorko, H. M., and Eckstein, F. (1984) *J. Biol. Chem.* 259, 13037–13040.
- Hurwitz, J., Weissbach, A., Horecker, B. L., and Smyrniotis, P. Z. (1956) *J. Biol. Chem.* 218, 769–783.
- Porter, M. A., Stringer, C. D., and Hartman, F. C. (1988) *J. Biol. Chem.* 263, 123–129.
- Porter, M. A., and Hartman, F. C. (1990) *Arch. Biochem. Biophys.* 281, 330–334.
- Brandes, H. K., Larimer, F. W., and Hartman, F. C. (1996) *J. Biol. Chem.* 271, 3333–3335.
- Sandbaken, M. G., Runquist, J. A., Barbieri, J. T., and Miziorko, H. M. (1992) *Biochemistry* 31, 3715–3719.
- Roesler, K. R., Marcotte, B. L., and Ogren, W. L. (1992) *Plant Physiol.* 98, 1285–1289.
- Charlier, H. A., Runquist, J. A., and Miziorko, H. M. (1994) *Biochemistry* 33, 9343–9350.
- Runquist, J. A., Harrison, D. H. T., and Miziorko, H. M. (1998) *Biochemistry* 37, 1221–1226.
- Harrison, D. H. T., Runquist, J. A., Holub, A., and Miziorko, H. M. (1998) *Biochemistry* 37, 5074–5085.
- Pai, E. F., Sachsenheimer, W., Schirmer, R. H., and Schulz, G. E. (1977) *J. Mol. Biol.* 114, 37–45.
- Schlauderer, G. J., Proba, J. A., and Schulz, G. E. (1996) *J. Mol. Biol.* 256, 223–227.
- Müller-Dieckmann, H. J., and Schulz, G. E. (1995) *J. Mol. Biol.* 246, 522–530.
- Hasemann, C. A., Istvan, E. S., Uyeda, K., and Deisenhofer, J. (1996) *Structure* 4, 1017–1029.
- Runquist, J. A., Harrison, D. H. T., and Miziorko, H. M. (1999) *FASEB J.* 13, A1353.
- Runquist, J. A., Narasimhan, C., Wolff, C. E., Koteiche, H. A., and Miziorko, H. M. (1996) *Biochemistry* 35, 15049–15056.
- Bradford, M. (1976) *Anal. Biochem.* 72, 248–254.
- Paulsen, J. M., and Lane, M. D. (1966) *Biochemistry* 5, 2350–2357.
- Marquardt, D. W. (1963) *SIAM J. Appl. Math.* 2, 431–441.
- Perrella, F. W. (1988) *Anal. Biochem.* 174, 437–447.
- Gibson, J. L., and Tabita, F. R. (1987) *J. Bacteriol.* 169, 3685–3690.
- Porter, M. A., Milanez, S., Stringer, C. D., and Hartman, F. C. (1986) *Arch. Biochem. Biophys.* 245, 14–23.
- Krieger, T. J., and Miziorko, H. M. (1986) *Biochemistry* 25, 3496–3501.
- Miziorko, H. M., Brodt, C. A., and Krieger, T. J. (1990) *J. Biol. Chem.* 265, 3642–3647.
- Koteiche, H. A., Narasimhan, C., Runquist, J. A., and Miziorko, H. M. (1995) *Biochemistry* 34, 15068–15074.
- Rippa, M., Spanio, L., and Pontremoli, S. (1967) *Arch. Biochem. Biophys.* 118, 48–57.
- Gardemann, A., Stitt, M., and Heldt, H. W. (1983) *Biochim. Biophys. Acta* 722, 51–60.
- Shirikihara, Y., and Evans, P. R. (1988) *J. Mol. Biol.* 204, 973–994.
- Adams, M. J., Ellis, G. H., Gover, S., Naylor, C. E., and Phillips, C. (1994) *Structure* 2, 651–668.
- Mizuguchi, H., Cook, P. F., Hasemann, C. A., and Uyeda, K. (1997) *Biochemistry* 36, 8775–8784.
- Brandes, H. K., Larimer, F. W., Lu, T. Y., Dey, J., and Hartman, F. C. (1998) *Arch. Biochem. Biophys.* 352, 130–136.
- Dahnke, T., Shi, Z., Yan, H., Jiang, R. T., and Tsai, M. D. (1992) *Biochemistry* 31, 6318–6328.
- Schlichting, I., and Reinstein, J. (1997) *Biochemistry* 36, 9290–9296.
- Admiraal, S. J., and Herschlag, D. (1995) *Chem. Biol.* 2, 729–739.
- Somerville, C. R., and Somerville, S. C. (1984) *Mol. Gen. Genet.* 193, 214–219.

BI9910326